



Tan, D. H. A., Seow, C. K. and Wen, K. (2022) Multi-Sensor Based IoT Indoor Localization. In: 2021 IEEE International Conference on Networking, Sensing and Control (ICNSC), Xiamen, China, 3-5 December 2021, ISBN 9781665440486 (doi: [10.1109/ICNSC52481.2021.9702235](https://doi.org/10.1109/ICNSC52481.2021.9702235))

The material cannot be used for any other purpose without further permission of the publisher and is for private use only.

There may be differences between this version and the published version. You are advised to consult the publisher's version if you wish to cite from it.

<http://eprints.gla.ac.uk/278268/>

Deposited on 01 September 2022

Enlighten – Research publications by members of the University of
Glasgow

<http://eprints.gla.ac.uk>

Multi-Sensor Based IoT Indoor Localization

De Hui Adrian Tan
School of Computing Science
University of Glasgow
Glasgow, United Kingdom
2427239T@student.gla.ac.uk

Chee Kiat Seow
School of Computing Science
University of Glasgow
Glasgow, United Kingdom
CheeKiat.Seow@glasgow.ac.uk

Kai Wen
School of Electrical and Electronic Engineering
Nanyang Technological University
Singapore, Singapore
we0001ai@e.ntu.edu.sg

Abstract—A typical indoor localization system relies on the availability of infrastructure such as Wi-Fi Access Points, blue-tooth beacons or antenna arrays. This increases the overall system cost and it may not be feasible for deployment in real environments such as shopping malls. A practical indoor localization system should be one that can function with minimum existing infrastructure. The proposed system in this paper leverages on the embedded sensors in off-the-shelf Internet of Things (IoT) devices such as smartphone in conjunction with Quick Response (QR) codes which are widely deployed under the authorities requirement due to COVID-19 pandemic. Our proposed stationary inertial measurement unit (IMU) feature is implemented through a first order finite impulse response (FIR) filter that works along with the QR codes. It has successfully reduced the drift errors suffered by IMU. The performance was evaluated in the testing environment at an university campus. From the evaluation results, the proposed method outperformed the conventional method (IMU only) and hybrid model (IMU + QR code) by 94.9% and 57.7% respectively, making the proposed method a promising technique that can be readily applied to other indoor environments.

Index Terms—inertial measurement unit (IMU), Quick Response (QR) code, finite impulse response (FIR) filter, indoor localization and navigation, Internet of Things (IoT)

I. INTRODUCTION

In current days, location-based services (LBS) have become an important part of people's daily lives. Global Positioning Systems (GPS) has been utilised extensively for outdoor localization purposes for decades. The applications using GPS do not provide a satisfactory result for indoor localization. With the recent advancement of Internet of Things (IoT) sensors and devices such as smartphone, indoor localization has become a key enabling technology for IoT applications to meet demands for LBS in indoor environments such as indoor navigation, marketing purposes, entertainment and information retrieval in an indoor context. Most indoor localization systems are implemented with various technologies such as Wi-Fi [1], [2], Line of Sight based (LOS) [3] and Non-LOS based identification [4]–[6], Bluetooth Low Energy (BLE) beacons [7], Ultra-wide band (UWB) [8], [9], Radio Frequency Identification [10], [11], Geomagnetic field and Inertial measurement unit [12]–[14]. This various indoor localization approaches produces multiple sets of small positioning data, which can be consolidated into a main server via 5G technology. These data can then be analyzed for purposes such as producing a big data heat-map to trace the movement of people in

an indoor location such as in a building or shopping mall. These various technologies however incur high costs due to the need for additional infrastructure to be present and also suffers from various different problems. In [15], a Wi-Fi based indoor positioning system with an improved hybrid ToA/AoA mechanism has been proposed by applying a round-trip time approach to obtain the distance without requiring time synchronization between transmitter and receiver. Even though the proposed method in [15] can reduce the number of antennas with superior performance improvement, the heavy reliance on nearby anchors still remains and hence increases the cost of deployment. Similarly, there is a limitation of available spaces to deploy nearby anchors which leads to the accuracy of the system being affected [15]. In [16], a Bluetooth based approach is implemented. Two novel approaches namely the Low-Precision (LIL) and High-Precision (HIL) Indoor localization with RSSI have been compared with the HIL approach having much higher accuracy. However, it still relies heavy on the Received Signal Strength Indicator (RSSI) measurements which is susceptible to multi-path fading that can cause signal fluctuation in the RSSI readings [16].

In [17], Poulouse et al. proposed an indoor positioning estimation algorithm relying on smartphone Inertial Measurement Unit (IMU) sensors data to implement a Pedestrian Dead Reckoning (PDR) algorithm. It leverages firstly on the IMU's 3D accelerometer and gyroscope data with a kalman filter to estimate the pitch and roll. It then performs step detection using the pitch estimation followed by a step length estimation through a first-order linear regression model on the pitch amplitude. The heading of the smartphone is then derived from the gyroscope and magnetometer values and passed through a noise removal kalman filter. The two components namely the step length and the orientation are then fused to estimate user's position. Even though the results show promising accuracy as compared to conventional methods, the proposed method still suffers from accumulating drift error [17] which is one of the shortcomings on using IMU for navigation.

Hybrid approaches have also been suggested to resolve indoor positioning problems. In [18], Chirakkal et al. proposed a QR based assistance approach with smartphone IMU to perform indoor localization. Its PDR algorithm makes use of the filtered sensor values to perform step detection and step length estimation to estimate the user's location. The QR

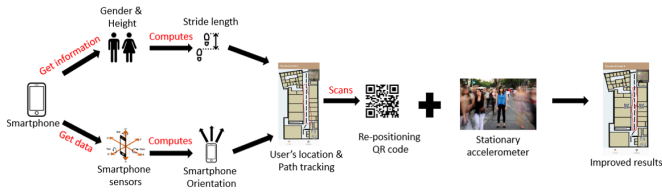


Fig. 1: Proposed method architecture

code is then used as an error compensator to the drift errors suffered by the IMU. The smartphone is equipped with a blueprint of the building. It utilizes a database to store the QR code's location with respect to the blueprint. While walking, the application will detect the nearest QR code and prompt the user to scan the code and hence correct the user's drift position. However, even with a much lower average error rates as compared to conventional approaches, the distance between each placed QR code is significantly short, forcing the user to scan the QR code frequently [18]. The need to scan multiple QR codes over a short distance is neither user-friendly nor resource effective as it drains smartphone battery whenever a scan is performed.

In order to reduce the required number of scans, this paper proposed a novel stationary IMU feature through a first order finite impulse response (FIR) filter that leverages on the smartphone IMU sensors in conjunction with QR codes. As the smartphone sensors suffer from an accumulating drift error over time, the proposed method using stationary IMU feature during movement pause period and QR code scanning at reference locations has outperformed conventional method (IMU only) and hybrid method (IMU + QR code) by 90.9% and 41.3% respectively. Our novel stationary IMU feature also managed to reduce the number of QR code deployed in the area compared to current hybrid method. This rest of this paper is organized as follows. Section II outlines the system overview of the proposed method while Section III explains the experiment set up and evaluation followed by conclusion and future work in Section IV.

II. SYSTEM OVERVIEW

The proposed system and architecture which is developed using the Android's operating system is shown in Figure 1. It consists of various components namely, PDR, QR code scanning as well as the proposed stationary IMU feature that is implemented using first order FIR. The localization of the user will be done via the PDR methodology with the stride length calculation, step detection algorithm and the orientation of the smartphone device. The QR code is used to determine the initial location of the user and serves as resetting mechanism to counteract against the drift error caused by the smartphone sensors by re-positioning the user. On the other hand, the proposed stationary IMU feature prompts the user to perform a momentary pause for n seconds to allow for the sensors to be reset. This is computed through a first order FIR filter.

A. Quick Response Code

The QR codes in the proposed method consists of two different types – initial QR code and re-positioning QR code. The initial QR code is encoded with an initial keyword, followed by the starting 2D location coordinates (x, y) and the floor level of the evaluated building. It provides the user's initial location and marks his/her entry into the building. This now becomes a standard implementation for every shopping mall and office building in Singapore due to the outbreak of COVID-19 virus. The re-positioning QR code is encoded with the re-positioning keyword, followed by the corresponding respective 2D coordinates (x, y) at that location. Upon scanning this QR code, the user will be re-positioned onto the correct location. This is also implemented at each store's entrance in all shopping malls. The keyword encoded in both QR codes aids in differentiating against the initial and the re-positioning QR code.

B. Stride length estimation

Everyone's stride length can vary due to several factors such as height, gender, age, injury, illnesses or terrains. In the proposed method, information provided by the user such as their gender, height and a constant that will be used to compute the stride length. The constant varies for different gender and is derived empirically. The formula for estimating stride length is as follows [19]:

$$\sigma = \frac{\eta\kappa}{2.54} \quad (1)$$

where σ is the stride length, η is the height input by the user and κ is a constant parameter according to the gender of the user. The value 2.54 cm is used as we need to calculate the pixel density or dots per inch (DPI). The model used in (1) is suffice for the experimental campaign in this paper. However, a more general and elaborated stride length parameter estimation can be further developed in future work. Another way to estimate the stride length is to use real-time accelerometer readings and calibrated step constant parameter [20]. This method requires less empirical data and is adjusted to the real time user acceleration. However this method needs monitored calibration process which is less practical compared to [19]. In fact, both [19] and [20] has similar performance when user is assumed to hold the smartphone in hand at normal walking pace and does no other unusual actions such as jumping during walking. Hence the method in [19] is used in this paper.

C. Step Detection Algorithm

For the proposed method, a step detection algorithm was applied to perform step counting to determine the stride. The base values for the step detection algorithm arises from the raw accelerometer sensor. When a person is walking, there is a spike pattern in the raw accelerometer readings. The readings are very crude and hence there is a need to smooth out the line by passing the raw linear accelerometer measurements through

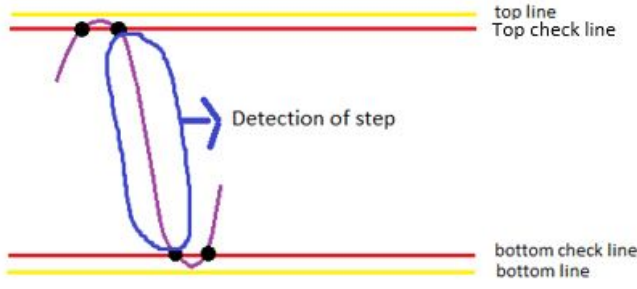


Fig. 2: Step condition detection

a low pass filter with a pre-selected cutoff frequency at nyquist frequency via the following formula [21]:

$$v[i] = f[i] + \delta(v[i-1] - f[i]) \quad (2)$$

where $v[i]$ is the output accelerometer values at time instance i after going through the low pass filter, $v[i-1]$ is the previous output accelerometer values and $f[i]$ is the input accelerometer values before going through the low pass filter. The δ is the pre-selected cutoff frequency and was chosen to be 0.9.

To detect each step phase, the algorithm will maintain four different thresholds defined by top line, top check line, bottom check line and bottom line. Figure 2 shows the threshold and acceleration value over time. The walking motion can be split into a transient phase, a lifting phase and a stepping phase. A transient phase is the phase in between the lifting and stepping phase. Lifting phase occurs when the user lifts his/her leg off the ground. The lifting of the leg will cause a synchronised movement to the user's hand as well. This motion of lifting is against the gravity and thus will arise a negative acceleration value which passes through the lower threshold. When the user put his/her leg down, the stepping phase will be activated and this result an alignment with gravitational force. Hence, it produces a positive acceleration value which passes through the upper threshold. The step detection algorithm detects that a step is taken when the value of the acceleration goes downwards through the upper threshold which is from a stepping phase towards transient phase which is denoted in Figure 2.

D. Orientation of device

The orientation computation of the smartphone device is based on the accelerometer and magnetometer's sensor values. As the sensors reside within the smartphone itself, it makes use of the local coordinate systems (LCS) as shown in Figure 3. However, in order to translate the smartphone's LCS to a global coordinate system (GCS), a coordinate transformation must be performed. The transformation is accomplished by the rotations about the X , Y and Z axes shown in Figure 3. When the smartphone is being held with screen facing upwards. The rotations can be represented in Euler angles and a rotation matrix is a convenient manner to represent and

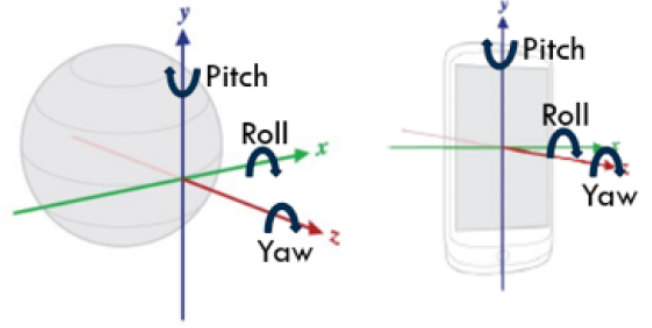


Fig. 3: Global coordinate system (left) and smartphone local coordinate system (right)

describe these rotations. The rotation matrices along each of the axes at time t are as follows [13]:

$$R_t = R_{\psi,t} R_{\theta,t} R_{\phi,t} = \begin{bmatrix} c\psi c\phi - s\psi s\theta s\phi & -s\psi c\theta & c\psi s\phi + s\psi s\theta c\phi \\ -s\psi c\phi - c\psi s\theta s\phi & -c\psi c\theta & -s\psi s\phi + c\psi s\theta c\phi \\ -c\theta s & s\theta & c\theta c\phi \end{bmatrix} \quad (3)$$

where c stands for \cos and s stands for \sin functions, roll = ϕ = rotation angle about X denoted by $R_{\phi,t}$, pitch = θ = rotation angle about Y denoted by $R_{\theta,t}$, and yaw = ψ = rotation angle about Z denoted by $R_{\psi,t}$.

These Euler angles are called roll, pitch and yaw respectively. The rows of rotation matrices are the projections of GCS on LCS and the columns are those of LCS on GCS. One of the main properties of the rotation matrices is its orthogonality. This means that any pair of the columns or rows in the matrix is perpendicular and the sum of all squares of the element in each column or row is unity. Using Android's `getRotationMatrix` method, it computes the inclination matrix I and the rotation matrix R by transforming a vector from the smartphone LCS coordinate system to the GCS which is being defined as a direct orthonormal basis. With the rotation matrix (R) computed from the `getRotationMatrix` formula, the rotation matrix R is used in the Android's `getOrientation` method which computes the orientation of the device and returns an array of values with the first value being the azimuth, angle of rotation around the Z axis, the second value being the pitch which is the angle of rotation around the Y axis and the third value being the roll which is the angle of rotation around the X axis. The azimuth values is used to determine the smartphone's orientation as the azimuth angle defines the angle between a celestial body (sun, moon) and the north, measured clockwise around the observer's horizon. It determines the direction of the celestial body. Hence, using the azimuth value determines the angle of the smartphone and then determines the direction the smartphone is pointing towards to.

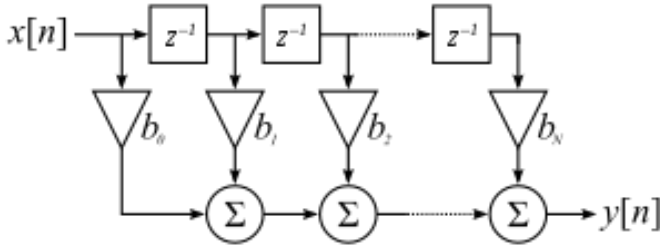


Fig. 4: Finite impulse response filter [21]

E. Stationary IMU

The novelty of this proposed method is the proposed stationary IMU feature that overcomes the IMU drift while at the same time reduces the leverage on QR code. As the smartphone embedded IMU sensors suffer from accumulating drift error over time, QR code will be required to counter act against the drift and re-position the user. However, to scan the QR code unless mandatory at shorter intervals may be more of a hassle than an aid which is not practical. In order to counter this issue, the momentarily stationary accelerometer can help to remove the drift. This can be achieved by prompting the user for momentary pause to allow for the accelerometer sensor to reset before proceeding to next movement. Hence, this allows the minimization on the reliance of QR code to reset the drift since the QR code may not be in visual view of the user. There are two types of momentary pause. The first type is the pause when user stopped at QR code's location and perform the scanning action. The user normally hold smartphone steady when perform scanning option. The other type of pause happens when the user is prompted to pause if there is no QR scanning action after walking for a period of time to allow the sensor to be reset. The moving period between pauses is flexible and it can be set as an input by user. In general it should be under 60 seconds depending on the scenarios to ensure accurate localization result. The pause duration is designed to be the same for both pause types and their start can be detected via the proposed stationary IMU feature with FIR filter described below.

The stationary IMU feature is developed using a first order FIR filter as shown in Figure 4 where $N = 1$. A FIR filter is a filter whose impulse response is of finite duration because it settles to zero in finite time. The output of the FIR filter can be calculated via the following:

$$\begin{aligned} \gamma[\tau] &= \beta^T \mathbf{a} \\ \beta &= [(1 - \omega), \omega]^T \\ \mathbf{a} &= [f[\tau], f[\tau - 1]]^T \end{aligned} \quad (4)$$

where τ is the filter time, $\gamma[\tau]$ is the output value, $f[\tau - 1]$ and $f[\tau]$ are previous and current accelerometer reading shown in (2), ω is value of impulse response at $\tau - 1$ time instant.

In the proposed method context, ω is set to a value of 0.9, placing a higher weight on the previous accelerometer reading value, $\zeta[\tau - 1]$. When the user enters the momentary pause, the FIR starts to work at $\tau - 1 = 1$ second with a weight of 0.9 while the weight of 0.1 is applied at $\tau = 2$ second. The user is required to stop for n seconds. At $\tau = n - 1$ second, the accelerometer value is 0 as there is no acceleration due to the fact that the user is not moving while at $\tau = n$ second, the user may start to have some undesired motion. With the ω being set to 0.9, the weight of the previous accelerometer value reading is heavier, implying that the previous reading value will influence the output value more than the current reading value. Hence FIR filter will help to mitigate the effect of undesired motion and smooth out noise from the beginning to the end of pause period.

III. EXPERIMENTS AND EVALUATION

To evaluate the performance and accuracy of the proposed algorithm, we conducted an experimental campaign on the proposed method with existing algorithms in the campus building as shown in Figure 5. The data collected are from the campus building at level 2 and 4. During the experiments, the user held the smartphone device in his hand and walked according to the reference path as shown in Figure 5 where the dashed lines serve as references. Single and multiple loops around the reference line are covered by users for localization performance comparison. Level 2 consists of multiple discussion rooms which contained students alongside with laptops and various devices. There are two lifts, one at the front and one at the back of the level. Level 4 consists of various laboratories containing multiple magnetic devices. There are also two lifts in level 4, one in the front and one at the back. Before conducting the experiments, an external application was used to measure the level of electromagnetic interference (EMI) in level 2, level 4. From Figure 6, electromagnetic field strength fluctuates in indoor environment due to the presence of magnetic objects in the vicinity. Such magnetic



Fig. 5: Campus building level 2 (left) and campus building level 4 (right)

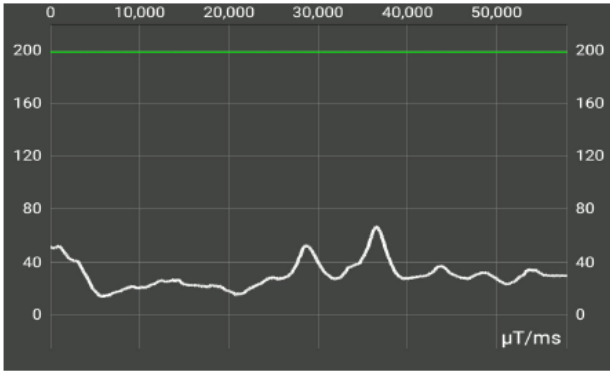


Fig. 6: EMI readings in indoor environment

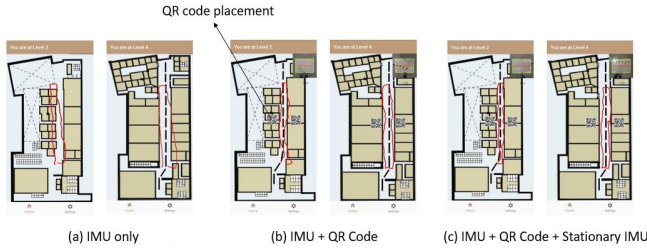


Fig. 7: Experiment results - Single loop

objects produces changing electrical currents and voltages that can cause EMI and affects the smartphone sensors which can cause drift errors. Therefore, this necessitates the need to reset the IMU sensors constantly. The proposed method of using IMU with QR code and the novel stationary IMU feature was compared against two conventional methods with minimum infrastructure - IMU only approach [17] and IMU with QR Code approach [18] under a straight walking path as well as single and multiple loops experiments. The real-time IMU measurements for different methods are carried out sequentially. As a result, the measurements are different even though the walking trajectories remain the same. Hence multiple loops are introduced to fairly evaluate localization performance despite the measurement differences. In our experiment, a 5 seconds momentary pause is imposed to ensure the user stops completely in order for the FIR filter to work as intended. Figures 7 and 8 show that the usage of QR code increases the accuracy of the IMU only approach in terms of lower drift error suffered. The effect of the stationary IMU feature in the proposed method is very evident in the multiple loop experiment conducted shown in Figure 8 as the results show a more consistent trajectories as compared to conventional method with just QR code.

From Figures 9 and 10, it can be seen that the introduction of the stationary IMU is able to produce better accuracy results since the IMU sensors are reset during the stationary period. The overall drift errors are calculated by the total deviation of the calculated trajectories from the true one over the span of 100 m and 600 m in a single and multiple loops respectively,

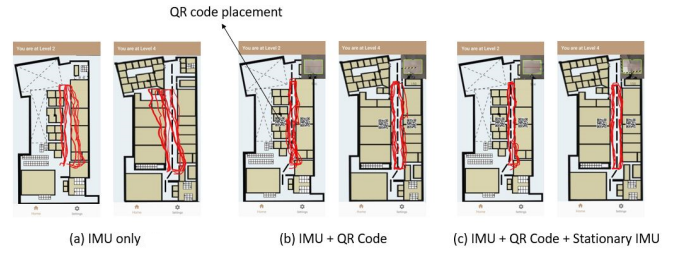


Fig. 8: Experiment results - Multiple loops

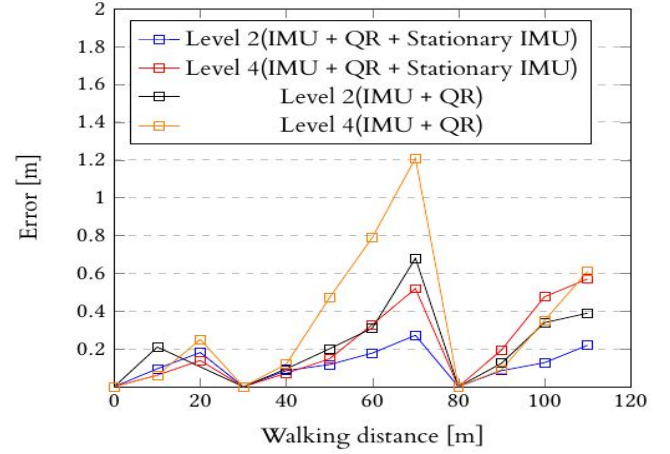


Fig. 9: Comparison of conventional approach with QR Code against proposed method - single loop

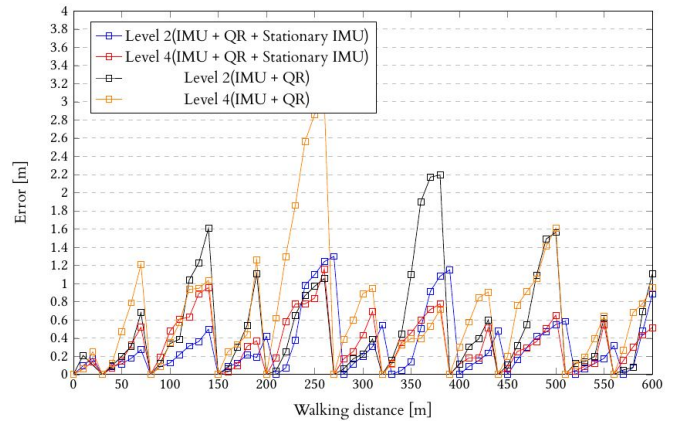


Fig. 10: Comparison of conventional approach with QR code against proposed method - multiple loops

which can be calculated via the following:

$$\|\epsilon\|_2 = \left[\sum_{i=0}^{\ell} (x_i^o - x_i)^2 + (y_i^o - y_i)^2 \right]^{1/2} \quad (5)$$

where (x_i^o, y_i^o) and (x_i, y_i) are the true and measured position coordinates provided by existing/proposed localization algorithm respectively, ℓ is the distance of 100 m and 600 m for single and multiple loops respectively and i is the measured points from start to end with 1 meter interval.

Level 2/4	Single Path/Single/Multi Loop	Compare against With/Without QR code	Improvement in %
L2	Single Path	Without QR Code	87.65
L4	Single Path	Without QR Code	90.97
L2	Single Loop	Without QR Code	94.88
L4	Single Loop	Without QR Code	87.4
L2	Multi Path	Without QR Code	45.9
L4	Multi Path	Without QR Code	58.6
L2	Single Path	With QR Code	41.35
L4	Single Path	With QR Code	36.4
L2	Single Loop	With QR Code	42.9
L4	Single Loop	With QR Code	36.6
L2	Multi Path	With QR Code	35.6
L4	Multi Path	With QR Code	57.7

Fig. 11: Improvement of proposed method compared against existing approaches

When the user is prompted to perform momentary pause, the sensor values drops to a 0 sequentially aligning to a stationary IMU. Single path is defined as the path from starting point to the returning point in one loop. Multiple path is the repetition of the single straight path multiple times. Based on the results garnered from the experiments, the accuracy improvements can be computed as shown in the table in Figure 11. With the proposed method, results show maximum accuracy improvement of proposed method (Stationary IMU + QR Code) by 94.9% - level 2 (91.0% - level 4) and 42.9% - level 2 (57.7% - level 4) over conventional method (IMU only) and hybrid method (IMU + QR code), respectively.

IV. CONCLUSION AND FUTURE WORK

This paper has proposed a low cost novel stationary IMU feature with QR code for indoor localization using smartphone embedded sensors with minimum extra infrastructure. The proposed stationary IMU feature not only outperformed existing algorithms by 94.9% and 57.7% as compared with conventional method (IMU only) and hybrid model (IMU + QR code) respectively. It helps to extend the distance between each placed QR code in strategic locations and highlights the practicality of the proposed method implementation since substantial amount of QR codes are deployed after the outbreak of COVID-19 pandemic globally for safe entry check. In future, the proposed method can also be evaluated at more complex indoor environments including shopping malls. Augmented and virtual reality with the Field of Vision (FOV) can also be introduced to detect the most optimal angle of user scanning the QR code navigation.

REFERENCES

- [1] M. Zhou, X. Geng, Q. Pu, X. Huang and Y. Wang, "An Analysis towards Synergetic Test of Wi-Fi Signal for Indoor Localization," 2019 IEEE 30th Annual International Symposium on Personal, Indoor and Mobile Radio Communications (PIMRC), Istanbul, Turkey, pp. 1-6, 2019.
- [2] M. N. Husen and S. Lee, Indoor location sensing with invariant Wi-Fi received signal strength Fingerprinting, *Sensors*, vol. 16, no. 11, pp. 1898, 2016.
- [3] C.K. Seow and S.Y. Tan, "Localisation of mobile device in multipath environment using bi-directional estimation", *IET Electronics letters*, vol. 44, no. 7, pp 485-487, 2008
- [4] S.W. Chen, C.K. Seow and S.Y. Tan, "Elliptical Lagrange-based NLOS Tracking Localization scheme", *IEEE Transactions on Wireless Communications*, vol. 15, no. 5, pp 3212-3225, 2016

- [5] S.W. Chen, C.K. Seow and S.Y. Tan, "Single reference mobile localization in multipath environment", *IET Electronics letters*, vol. 49, no. 21, pp 1360-1362, 2013
- [6] H. Zhang, S.Y. Tan and C.K. Seow, "TOA-based indoor localization and tracking with inaccurate floor plan map via MRMSC-PHD filter, *IEEE Sensors Journal*, vol. 19, no. 21, pp.9869-9882, 2019
- [7] J. H. An and L. Choi, "Inverse fingerprinting: Server side indoor localization with Bluetooth low energy," 2016 IEEE 27th Annual International Symposium on Personal, Indoor, and Mobile Radio Communications (PIMRC), Valencia, pp. 1-6, 2016.
- [8] G. Selimis, J. Romme, H. Pflug, K. Philips, G. Dolmans and H. de Groot, "Sub-meter UWB localization: Low complexity design and evaluation in a real localization system," 2013 IEEE 24th Annual International Symposium on Personal, Indoor, and Mobile Radio Communications (PIMRC), London, 2013, pp. 186-191.
- [9] A.R. Jimenez and F. Seco, Comparing decawave and bespoon UWB location systems: Indoor/outdoor performance analysis, in *Proc. Indoor Positioning Indoor Navigation (IPIN)*, pp. 1-18, Oct 2016.
- [10] F. Seco, A. R. Jiménez, "Smartphone-based cooperative indoor localization with RFID technology," *Sensors*, vol. 18, no. 1, pp. 266, Jan. 2018.
- [11] J. Huang and X. Yu, Y. Wang and X. Xiao, An integrated wireless wearable sensor system for posture recognition and indoor localization, *Sensors*, vol. 16, no. 11, pp. 1825, 2016.
- [12] K. Wen, C. K. Seow, S. Y. Tan, "Inertial navigation system positioning error analysis and Cramér-Rao lower bound, " in *Proc. IEEE/ION Position Location and Navigation Symposium (PLANS'16)*, 2016, pp. 213-218.
- [13] K. Wen, C.K. Seow, S.Y. Tan, "An indoor localization and tracking system using successive weighted RSS projection," *IEEE Antennas and Wireless Propagation Letters*, vol. 19, pp. 1620-1624, Sep 2020.
- [14] W. Sakpere, M. Adeyeye Oshin and N. B. Mlitwa, A State-of-the-Art Survey of Indoor Positioning and Navigation Systems and Technologies, *South African Computer Journal*, vol. 29, no. 3, pp.145-197, 2017.
- [15] Chouchang Yang and Huai-Rong Shao, WiFi-Based Indoor Positioning, *IEEE Communications Magazine*, pp. 150-156, Mar 2015.
- [16] Y. X. Wang and Q. Ye and J. Cheng and L. Wang, RSSI-based Bluetooth Indoor Localization, 11th International Conference on Mobile Ad-hoc and Sensor Networks, pp. 165-170, 2015.
- [17] A. Poulouse and D. S. Eyobu and D.S. Han, An Indoor Position-Estimation Algorithm Using Smartphone IMU Sensor Data, *IEEE Access*, vol. 7, pp. 11165-11175, 2019.
- [18] Chirakkal, Vinjohn and Park, Myung Chul and Han, Dong Seog, An Indoor Position-Estimation Algorithm Using Smartphone IMU Sensor Data, Exploring Smartphone-Based Indoor Navigation: A QR Code Assistance-Based Approach, *IEIE Transactions on Smart Processing and Computing*, vol. 4 pp. 1-2, June 2015.
- [19] Stride Length and Step Length, <https://www.healthline.com/health/stride-length>, Sep 2018.
- [20] H. Cho, Y. Kwon, "RSS-based indoor localization with PDR location tracking for wireless sensor networks," *AEÜ-International Journal of Electronics and Communications*, vol. 70, no. 3, pp. 250-256, Mar. 2016.
- [21] J. G. Proakis and D. G. Manolakis, *Digital Signal Processing: Principles Algorithms and Applications*, New York:Macmillan, 2007.